Hindawi
Advances in Civil Engineering
Volume 2019, Article ID 9641674, 16 pages
https://doi.org/10.1155/2019/9641674

Research Article

Study on the Design Method for the Deformation State Control of Pile-Anchor Structures in Deep Foundation Pits

Jinkun Sun,[1,2] **Senping Wang**,[1,2] **Xinjun Shi**,[2] **Feng Wu**,[2] **and Liyun Zeng**[2,3]

[1]*School of Civil Engineering and Environment, Xihua University, Chengdu 610039, China*
[2]*Civil and Architectural Engineering Institute, Panzhihua University, Panzhihua 617000, China*
[3]*Rattanakosin International College of Creative Entrepreneurship, Rajamangala University of Technology Rattanakosin, Bangkok 10700, Thailand*

Correspondence should be addressed to Jinkun Sun; paxf66290838@163.com

Received 19 May 2019; Revised 4 September 2019; Accepted 2 October 2019; Published 31 October 2019

Academic Editor: Valeria Vignali

At present, the design of pile-anchor structures for deep foundation pits can be divided into the limit state control design of the bearing capacity and the limit state control design in normal use (i.e., "deformation state control design"). Strength design focuses on the strength control of supporting structures and rock-soil masses, while deformation design focuses on the deformation and environmental impact control of supporting structures and rock-soil masses. However, since a rock-soil mass, especially a soil mass, is a rheid, the strength control design process is not completely reliable, and the deformation control design is also required when the rheological behavior is prominent. A pile-anchor structure can limit the deformation of supporting structures by applying a prestress, with good technical and economic benefits; therefore, it has been widely used in the support engineering of deep foundation pits. In this paper, the objective of the deformation state control of pile-anchor structures for deep foundation pits, the corresponding stress level thresholds, and the determination of the bearing capacity checkpoint are studied based on the strength parameters of the soil deformation state and by combining a theoretical calculation analysis of the stress mode of pile-anchor structures, the calculations of previous engineering cases, and finite element simulation. Based on the depth of the plastic zone of the soil in the built-in section of the foundation pit supporting the structure, the position of the deformation state checkpoint of the soil in the built-in section inside the foundation pit is determined as one-third of the length h_d of the built-in section below the bottom of the foundation pit; the stress level threshold $\lambda^{(2)}$ corresponding to the slow, steady state is determined as approximately 30%–60% based on the curve characteristics of the relationship between the deformation and the stress level of the soil in the built-in section $(1/3)h_d$ below the bottom of the foundation pit. Based on the stress mode and deformation control requirements of the anchorage section of the pile-anchor structure and the Mohr–Coulomb strength criterion, the deformation state control design method of the pile-anchor structure is constructed by taking the deformation state bearing capacity at $(1/3)h_d$ as the checkpoint and the stress level threshold $\lambda^{(2)}$ corresponding to the slow, steady state.

1. Introduction

Foundation pit support engineering is mainly used to protect the construction of underground main structures, to ensure environmental safety around foundation pits, and to provide temporary support, reinforcement, protection, and groundwater control measures for foundation pits. In addition, it provides the necessary construction space for the underground structures of various buildings. With increasing acceleration of urbanization, rapid development of underground space utilization, construction of urban subway squares and increasing excavation depth and scale of foundation pits, the difficulty of foundation pit engineering has become more prominent. Furthermore, these projects are often concentrated in urban areas, requiring strict control over the impact of the foundation pit deformation on surrounding buildings. Therefore, a deep foundation pit has the characteristics of a large excavation scale, substantial depth and strict deformation control. As the requirements for the displacement become increasingly strict, the

traditional design method of stability control can no longer meet the requirements of design and construction, and a series of technical systems and standards must be applied in terms of the construction concept, design method, construction technology and process, test technology and quality control.

In studies on the soil deformation state characteristics, the soil deformation state refers to the characteristics of the deformation state over time under different stress or load levels. Vyalov [1] classified three critical stresses based on the curve characteristics of the shear strain rate $d\gamma/dt$ and shear stress τ: the relative elasticity limit state τ_k, the relative flow limit state τ_r, and the complete failure state τ_f. Tan Tjongkie [2] proposed a stress threshold corresponding to a similar soil deformation state in view of the rheological curve characteristics of weak overconsolidated clay. Cai and Cao [3] analyzed the accumulated number of cumulative plastic deformation events under a load (the number of load events can be considered a variant expression of time) through a dynamic triaxial test of clay and concluded that the cumulative plastic deformation characteristics can be divided into two categories: development and attenuation. Werkmeister et al. [4] divided the cumulative plastic deformation into three stages from the viewpoint of stability: plastic stability, plastic creep, and incremental failure. Regarding studies on the determination method of the soil deformation state, Liu [5] described the relationship between the cumulative plastic deformation rate $f(N)$ and cycle number N, that is, $f(N) = CN^{-p}$, by using a negative power function; they also studied the evolution state of the long-term cumulative plastic deformation of coarse-grained soil under cyclic loading and divided the cumulative plastic deformation into four states, including fast stabilization ($p \geq 2$), slow stabilization ($1 < p < 2$), slow failure ($0 < p \leq 1$), and fast failure ($p \leq 0$), based on the influence law of the power p on the convergence and divergence of the negative power function. Xiong et al. [6], based on fractal theory, established a fractal relationship between the plastic deformation rate and time, proposed the "fractal dimension method," and divided the change in the soil deformation with the load level into fast stabilization and slow stabilization, and slow failure and fast failure. Regarding the application of soil deformation state theory, Xiong et al. [6] discussed a method for determining the thickness of the foundation compression layer for a non-highly compressible soil foundation based on soil deformation state control and concluded that for this type of foundation, the compressive layer thickness corresponds to the thickness determined by the stress ratio method as per $\psi = 0.2$. Li [7] established a design method for shoulder sheet pile walls based on the soil deformation state control and proposed that the corner threshold of anchor piles with fast and stable lateral displacement was approximately 0.1‰ rad for rigid anchor piles. In studies on the design method for deformation control of deep foundation pits, Terzaghi et al. [8] proposed a calculation method for excavation deformation and stability. Yao [9] proposed the deformation control concept for civil works. Liu et al. [10, 11] proposed construction methods such as "balance, symmetry, time limit" to control the deformation of foundation pits for soft soil areas in Shanghai. Liu et al. [12, 13] concluded that shortening the exposure time of the foundation pit soil was the key to controlling the displacement of supporting structures. Jia [14] combined the engineering practices of deep foundation pits in Shanghai to solve the deformation control problem of deep foundation pits in saturated soft clay areas. In summary, the current studies on the design method for deformation control of deep foundation pits are mainly based on the selection and rigidity of supporting structures, and the problem of time-dependent deformation of foundation pits cannot be effectively solved in the design stage of supporting structures of foundation pits and still requires an in-depth study.

In a pile-anchor structure for a deep foundation pit, the horizontal axial force of anchor rods (cables) can balance the partial earth pressure above the excavation surface outside the foundation pit, reduce the load level of the anchorage section of the supporting piles, and improve the deformation behavior of the supporting piles, thus achieving the purpose of controlling the lateral deformation of the foundation pit; therefore, this method has been widely used in deep foundation pit support engineering. However, the action of anchor rods (cables) also makes the stress and deformation of the supporting structure more complicated [15–17]. Research results in recent years have shown that [18, 19] the position of the anchor rods (cables) in a pile-anchor structure, the rigidity of the supporting structure, and the resistance coefficient of the foundation in the built-in section have a great impact on the stress and deformation characteristics of a pile-anchor structure. The traditional design method of pile-anchor structures consists mainly of solving the strength problem of the deep foundation pit soil but fails to effectively solve the deformation problem in the design stage. In the case of different excavation depths of a deep foundation pit, anchor piles produce horizontal deformation at different speeds over time, which directly affects the stability of the foundation pit and the safety of surrounding buildings. During construction, the early application of prestressed anchor cables increases the project cost, while excessively late application may lead to the destruction of the foundation pit. These technical and engineering problems lie at the core of pit pile-anchor structure design for deep foundation pits. The construction of deep foundation pits is characterized by a large quantity of engineering supplies and high cost and has become the key to managing project progress, guaranteeing project quality, and reducing project costs. Therefore, it is important to summarize the existing technical achievements of deep foundation pit support engineering, study the design method of pile-anchor structures for deep foundation pits based on deformation state control, and determine the checkpoint which plays a key role in the soil deformation state control of deep foundation pits and the stress level control of the soil in the anchorage section of anchor piles to provide a strong theoretical and practical reference for the design method of deformation control of deep foundation pits.

2. Basic Expression of the Deformation State Design Method

2.1. Basic Stress Model. The basic stress model can be established based on the stress characteristics of pile-anchor structures of deep foundation pits, as shown in Figure 1.

2.2. Expression of the Design Method

2.2.1. Earth Pressure E_a above the Excavation Surface of the Foundation Pit. The earth pressure strength e_{ai} and resultant force E_a above the excavation surface of the foundation pit are determined in accordance with JGJ120-2012 *Technical Specification for Retaining and Protection of Building Foundation Excavations*, as shown in

$$E_a = \sum_{n}^{i=1} e_{ai}. \tag{1}$$

2.2.2. Horizontal Reaction Force F_h of the Anchor Rod (Cable) Fulcrum. The horizontal reaction force F_h of the elastic fulcrum within the calculated width of the anchor rod (cable) is determined in accordance with JGJ120-2012 *Technical Specification for Retaining and Protection of Building Foundation Excavations*, as shown in

$$F_h = k_R (v_R - v_{R0}) + P_h, \tag{2}$$

where k_R is the stiffness coefficient of the fulcrum (kN/m), v_R is the horizontal displacement at the fulcrum (m), v_{R0} is the initial horizontal displacement of the fulcrum (m), and P_h is the normal prestressing in the calculated width of the retaining structure (kN).

2.2.3. Shear Force Q_0 and Bending Moment M_0 of the Supporting Pile at the Bottom of the Foundation Pit. The shear force and bending moment of the supporting pile at the bottom of the foundation pit are determined based on the earth pressure and resultant force E_a above the excavation surface of the foundation pit and the horizontal reaction force F_h of the anchor rod (cable), as shown in equations (3) and (4):

$$Q_0 = E_a b_a - \sum_{n}^{i=1} F_{hi}, \tag{3}$$

$$M_0 = E_a h b_a - \sum_{n}^{i=1} F_{hi} h_i, \tag{4}$$

where b_a is the horizontal spacing of the supporting pile (m).

2.2.4. Internal Force of the Built-in Section of the Supporting Pile. The internal force of the built-in section of the supporting pile is calculated by the elastic foundation beam method. The deformation differential equation of the elastic foundation beam given in Reference [15] is shown in equation (5), while the differential equation in References [20, 21] is shown in equation (6):

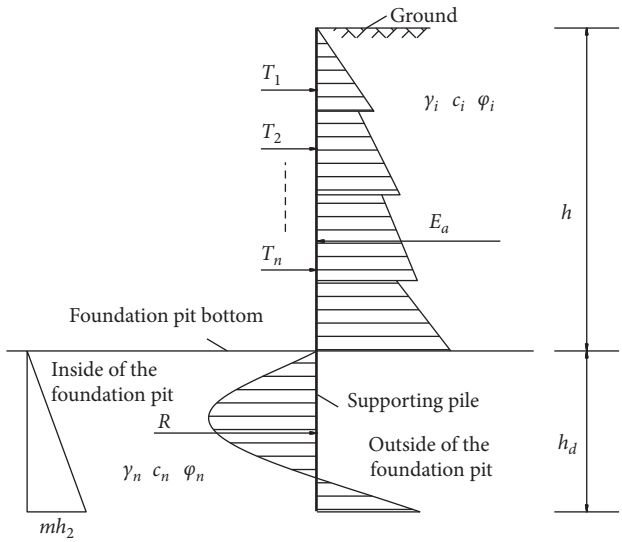

Figure 1: Stress mode diagram of a pile-anchor structure.

$$\mathrm{EI}\frac{\mathrm{d}^4 x}{\mathrm{d}y^4} + k_s x b_0 - e_a(z) = 0, \tag{5}$$

$$\mathrm{EI}\frac{\mathrm{d}^4 x}{\mathrm{d}y^4} + k_s x b_0 = 0, \tag{6}$$

where EI is the flexural rigidity of the pile (kN·m^2), k_s is the ground-level reaction coefficient (kN/m^3), b_0 is the calculated width of the pile (m), x is the horizontal displacement at the calculation point (m), $e_a(z)$ is the active earth pressure outside the foundation pit at the calculation point (kN/m).

The difference between equations (5) and (6) lies in whether the active earth pressure outside the foundation pit is included in the differential equation of deformation. This factor should be considered from the mechanism of the soil reaction. The fundamental cause of the soil reaction is the unbalanced force on both sides of the supporting pile. Under the action of the unbalanced force, the displacement of the elastic foundation beam causes soil deformation inside the foundation pit of the supporting piles, forming a reaction pressure, so the differential equation of the deformation of the elastic foundation beam has essentially taken into account the active earth pressure outside the foundation pit. In this regard, the differential equation of equation (6) is reasonable. Based on the power series solution of equation (6), the horizontal displacement x, rotation angle ϕ, bending moment M, and shear force Q at any cross-section of the pile body in the built-in section can be obtained as shown in the following equation:

$$\begin{cases} x = x_0 A_1 + \dfrac{\phi_0}{\alpha} B_1 + \dfrac{M_0}{\alpha^2 \mathrm{EI}} C_1 + \dfrac{Q_0}{\alpha^3 EI} D_1, \\ \phi = \alpha\left(x_0 A_2 + \dfrac{\phi_0}{\alpha} B_2 + \dfrac{M_0}{\alpha^2 \mathrm{EI}} C_2 + \dfrac{Q_0}{\alpha^3 \mathrm{EI}} D_2 \right), \\ M = \alpha^2 \mathrm{EI}\left(x_0 A_3 + \dfrac{\phi_0}{\alpha} B_3 + \dfrac{M_0}{\alpha^2 \mathrm{EI}} C_3 + \dfrac{Q_0}{\alpha^3 \mathrm{EI}} D_3 \right), \\ Q = \alpha^3 \mathrm{EI}\left(x_0 A_4 + \dfrac{\phi_0}{\alpha} B_4 + \dfrac{M_0}{\alpha^2 \mathrm{EI}} C_4 + \dfrac{Q_0}{\alpha^3 \mathrm{EI}} D_4 \right), \end{cases} \tag{7}$$

where A_i, B_i, C_i, and D_i are the coefficients determined under the boundary conditions.

2.2.5. Soil Reaction of the Built-in Section of the Supporting Pile inside the Foundation Pit. The soil reaction p_s of the built-in section is calculated by the "m" method, as shown in the following equation:

$$p_s = k_s x = myx, \tag{8}$$

where m is the proportionality coefficient of the soil reaction (kN/m^4) and y is the depth from the calculation point to the foundation pit bottom (m).

2.2.6. Bearing Capacity of the Soil Deformation State in the Built-in Section of the Foundation Pit. Based on the stress mode of the pile-anchor structure and the action mechanism of the soil reaction of the built-in section inside the foundation pit, it can be considered that the limit state of the soil reaction of the built-in section should be the passive earth pressure e_p in the built-in section of the foundation pit, as shown in the following equation:

$$p_{s\max} = e_p = \gamma y \tan 2\left(45^\circ + \frac{\varphi}{2}\right) + 2c \tan\left(45^\circ + \frac{\varphi}{2}\right). \tag{9}$$

Based on the deformation state strength parameter of equation (10) and the control objective that the soil in the built-in section inside the foundation pit is controlled in a slow stabilization state, the bearing capacity $p_s^{(2)}$ can be obtained when the soil deformation in the built-in section inside the foundation pit is in a slow stabilization state, as shown in the following equation:

$$p_s^{(2)} = \gamma y \tan^2\left(45^\circ + \frac{\varphi^{(2)}}{2}\right) + 2c^{(2)} \tan\left(45^\circ + \frac{\varphi^{(2)}}{2}\right), \tag{10}$$

where $c^{(2)}$ and $\varphi^{(2)}$ are strength parameters corresponding to the slow stabilization state.

2.2.7. Evaluation of the Deformation State of the Built-in Section inside the Foundation Pit. For the soil reaction p_s of the built-in section of the supporting pile calculated as per equation (9) and the bearing capacity $p_s^{(2)}$ calculated as per equation (10) when the soil deformation of the built-in section is in a slow stabilization state, if $p_s \le p_s^{(2)}$ at the checkpoint, the soil deformation is in a slow stabilization state.

3. Calculation and Analysis of Engineering Cases

3.1. Project Overview. The pile-anchor structure for deep foundation pits in a large-scale project is selected as a calculation example. In this project, the excavation depth of the foundation pit is 23.6 m, the length of the supporting pile is 8.9 m, and the groundwater level after dewatering is 24.1 m below the ground. There are four prestressed anchor cables, with an angle of 15° to the horizontal direction, a horizontal spacing of 2.2 m, a specification of $1 \times 7\varphi s15.2$, and a standard strength of 1860 MPa. The supporting pile is 1.2 m in diameter and is poured with C30 reinforced concrete, with the calculation cross-section shown in Figure 2. The main stratum distribution and physical and mechanical parameters are shown in Table 1, and the parameters of each anchor cable are shown in Table 2.

3.2. Analysis of the Results of an Example Calculation. The horizontal axial force of each prestressed anchor cable and the bending moment M_0 and shear force Q_0 of the supporting pile at the foundation pit bottom are calculated by the elastic fulcrum method, as shown in Table 3. Specifically, the proportionality coefficient m_1 of the soil reaction coefficient of the dense pebble layer is 2.8×10^4 kN/m^4, and the proportionality coefficient m_2 of moderately weathered mudstones is 4×10^4 kN/m^4.

According to equation (7) and assuming that the bottom of the supporting pile is hinged, the soil reaction and the lateral displacement of the supporting pile in the built-in section of the foundation pit can be calculated, as shown in Figure 3. The proportionality coefficient m of the soil reaction coefficient inside the foundation pit is taken as the conversion value of two soil layers, as shown in the following equation:

$$m = \frac{m_1 h_1^2 + m_2 (2h_1 + h_2) h_2}{h^2}, \tag{11}$$

where m_1 and m_2 are the proportionality coefficients of the soil reaction coefficients of the first and second soil layers, respectively, kN/m^4; h_1 and h_2 are the thickness of the first and second soil layers, respectively, m; and h is the built-in depth, m.

The proportionality coefficient m of the soil reaction coefficient between the dense pebble layer and the moderately weathered mudstone layer calculated from equation (11) is approximately 3.8×10^4 kN/m^4.

As seen from Figure 3, the soil reaction inside the foundation pit is nonlinearly distributed along the depth. The main action range of the soil reaction is approximately 5 m below the bottom of the foundation pit, the position of the maximum soil reaction is approximately 2 m from the foundation pit bottom, and the ratio of the soil reaction to the depth of the built-in section at 8.9 m is approximately 0.22.

If the shear stress τ and τ_f (in the state of complete failure) are expressed in dimensionless form, that is, $\lambda = \tau/\tau_f$, the physical meaning of λ is the shear stress level of the soil, and the difference in the shear stress level also represents the different deformation states of the soil. In practical engineering applications, the limit strength of the soil is generally expressed by Mohr's stress circle. According to Vyalov [1], the limit deviatoric stress in Mohr's stress circle is reduced as per the deviatoric stress level λ to obtain the strength parameters c^i and φ^i of the soil deformation state corresponding to the deviatoric stress level. Therefore, the deformation state strength parameters corresponding to the different stress levels λ_i of the built-in section inside the foundation pit are as shown in Table 4.

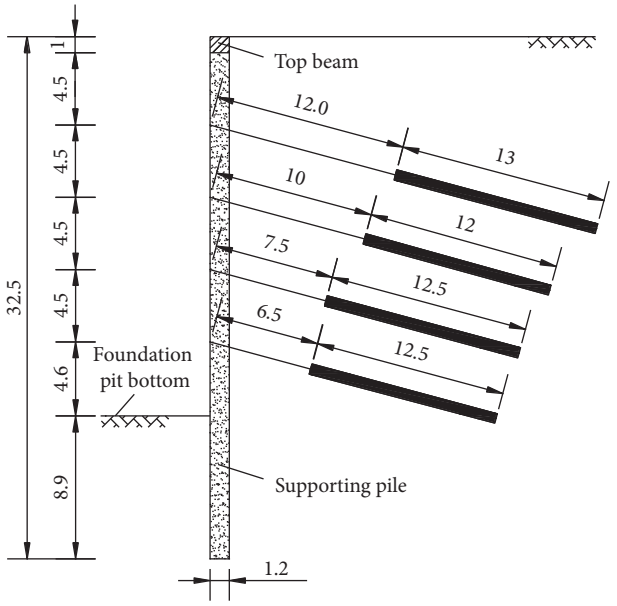

Figure 2: Diagram for calculation of the pile-anchor structure (unit: m).

Table 1: Physical and mechanical parameters of main stratum soil.

Soil layer	Thickness (m)	γ (kN/m^3)	c (kPa)	φ (°)	$E_{s1\text{-}2}$ (MPa)
Clay	8.6	19.0	38.4	19.1	6.5
Silty clay	1.6	19.1	21.7	20.0	5.8
Slightly medium-dense pebbles	4.8	22.0	—	31.0	17
Dense pebbles	13.5	23.6	—	40.0	40.0
Moderately weathered mudstones	—	24.7	300.0	33.0	—

Table 2: Parameters of each anchor cable.

Cable no.	Free section l_f (m)	Anchorage section l_a (m)	Prestress (kN)
1	12	13	300
2	10	12	350
3	7.5	12.5	350
4	6.5	12.5	300

Table 3: Axial force of anchor cable and internal force of supporting pile at the foundation pit bottom.

Cable no.	1	2	3	4
Horizontal axial force (kN)	451	691	792	574
Internal force of the supporting pile at the foundation pit bottom	Bending moment M_0	417 kN m		
	Shear force Q_0	730 kN		

According to the deformation state strength parameters in equation (10) and Table 4, the relationship between the soil deformation state bearing capacity $p_s^{(i)}$ of the built-in section and the soil reaction p_s of the built-in section of supporting pile is obtained as shown in Figure 4.

As seen from Figure 4, at a depth of 0–(1/3)h_d below the bottom of the foundation pit, the soil reaction inside the foundation pit reaches the passive earth pressure at the corresponding depth, forming a plastic zone with a stress level ranging from 30% to 100%; however, in the range of (1/3)h_d-h_d below the bottom of the foundation pit, the soil reaction is small and approximately equal to 0%–30% of the stress level λ_i.

3.3. Discussion on the Results of the Example Calculation and Determination of the Checkpoint. To further analyze the influence of the soil strength parameters on the stressing and deformation of the built-in section of the supporting pile under different stress levels, the internal friction angle φ is taken as a variable, as shown in Table 5, and the built-in section is composed of nonclayey soil of a single stratum. The curve of the relationship between the soil reaction of the built-in section of the supporting pile and the deformation state bearing capacity under different stress levels is obtained as shown in Figure 5.

As seen from Figure 5, as the internal friction angle φ decreases, the soil strength of the built-in section inside the foundation pit decreases, and the plastic zone of the soil in the built-in section gradually expands from (0–0.14)h_d below the bottom of the foundation pit to (0–0.34)h_d (h_d is the length of the built-in section). Nevertheless, from the view of the area of the distribution pattern of soil reaction and limit passive earth pressure, the resultant earth reaction p_s of the built-in section is still smaller than the resultant passive earth pressure E_p. For example, when φ is 15°, the resultant soil reaction p_s is approximately 680.7 kN/m, accounting for only 39% of $E_p \approx 1614.4$ kN/m. Thus, the requirement that "the resultant soil reaction shall not be greater than passive earth pressure" in JGJ120-2012 *Technical Specification for Retaining and Protection of Building Foundation Excavations* is not exhaustive or is ambiguous. On the premise of meeting this requirement, it is still necessary to limit the plastic zone development depth of the soil in the built-in section of the foundation pit, that is, the maximum development depth of the plastic zone shall not be greater than (1/3)h_d. In addition, (1/3)h_d can be taken as the checkpoint of the soil deformation state bearing capacity.

By taking the position (1/3)h_d below the bottom of the foundation pit taken as the soil deformation control position, the relationship between the earth reaction pressure p_s at (1/3)h_d and the corresponding stress level λ_i at different internal friction angles can be obtained based on the principle that the earth reaction pressure p_s is equal to the deformation bearing capacity $p_s^{(i)}$, as shown in Figure 6.

As seen from Figure 6, as the decrease in the internal friction angle φ decreases, the corresponding stress level of the soil reaction at (1/3)h_d below the bottom of the foundation pit gradually increases, and p_s decreases first and then decreases with an increasing stress level. The stress level corresponding to the maximum soil reaction is in the range of 30%–60%. According to the change trend of the lateral displacement and stress level of the supporting pile, the

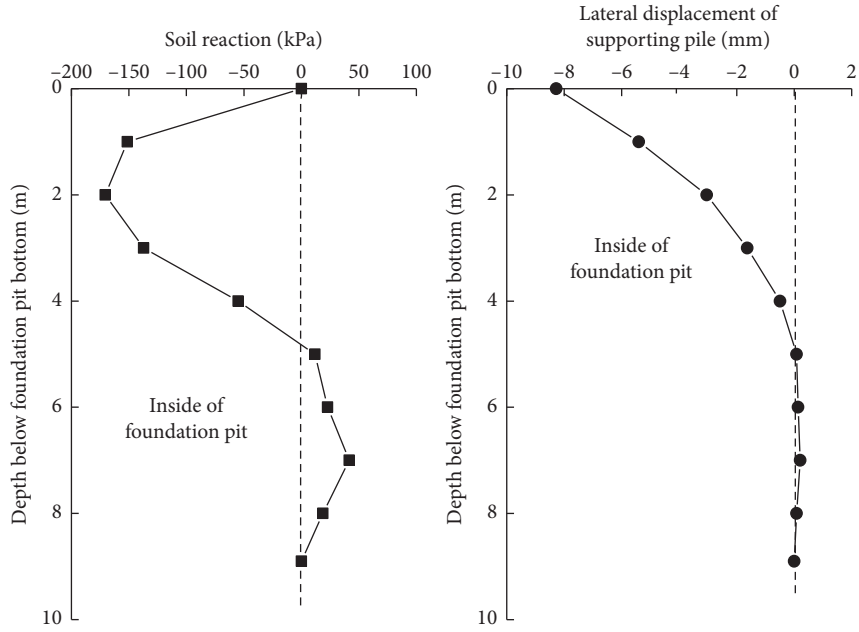

Figure 3: Soil reaction of the built-in section and lateral displacement of the supporting pile.

Table 4: Strength parameters of the soil deformation state corresponding to different stress levels.

Soil layer	λ_i	10%	20%	40%	60%	80%	100%
Dense pebbles	$c_1^{(i)}$ (kPa)	0	0	0	0	0	0
	$\varphi_1^{(i)}$ (°)	8.8	15.3	24.7	31.3	36.2	40
Moderately weathered mudstone	$c_2^{(i)}$ (kPa)	49.6	90.9	158	212.4	259	300
	$\varphi_2^{(i)}$ (°)	6.1	11.1	18.9	24.7	29.3	33

lateral displacement increases with increasing stress level, and when the stress level is more than 30%–60%, the range of the lateral displacement range is obviously increased. The curve of the pile lateral displacement and stress level has a characteristic point of curvature, which reflects the fundamental change in the lateral displacement of the pile. To further reflect the change in the pile lateral displacement with the stress level, the relation curve between the relative growth rate of the pile lateral displacement and the stress level can be obtained, as shown in Figure 7.

As seen from Figure 7, the relative growth rate of the pile lateral displacement increases rapidly when the stress level λ_i is equal to or greater than (30%–60%), reflecting that the soil deformation in the built-in section of the foundation pit tends to cause failure. Thus, when the stress level λ_i is (30%–60%), the soil deformation in the built-in section is in the critical state of slow stabilization and failure. This state is considered to coincide with the conclusion that the soil is in the critical state of slow stabilization when the stress level obtained by the indoor triaxial test, direct shear test and unit model test on the soil deformation state as carried out in references [6, 22, 23] is 30%–60%.

In this section, the variation law of depth with the stress level in the plastic zone of the soil in the anchorage section of the anchor pile is calculated and discussed through an engineering example, and the position of the checkpoint for the soil deformation state bearing capacity in the anchorage section is determined.

4. Numerical Simulation Analysis

4.1. Simulation Purpose and Parameter Selection. The finite element numerical analysis is used to further explain and verify the position of the checkpoint. The purpose of the finite element numerical analysis is to verify the variation law of the plastic zone development range at different internal friction angles of the soil in the built-in section, thus further verifying the unified combination of the plastic zone development depth and the position of the bearing capacity checkpoint of the soil deformation state and providing a reliable basis for checking the design calculations.

To verify the accuracy of the theoretical calculation, a numerical analysis is conducted using the Dutch Plaxis finite element program, and the results are compared with those of the theoretical calculation. The soil layer of the anchorage section is selected as the main soil for the model. The external load above the foundation pit bottom is equally applied to the upper part of the model. The parameters of the soil layer outside the foundation pit are shown in Table 6, and the mechanical parameters of the pile row are shown in Table 7. Different internal friction angles are considered for the soil inside the foundation pit. To avoid the deep

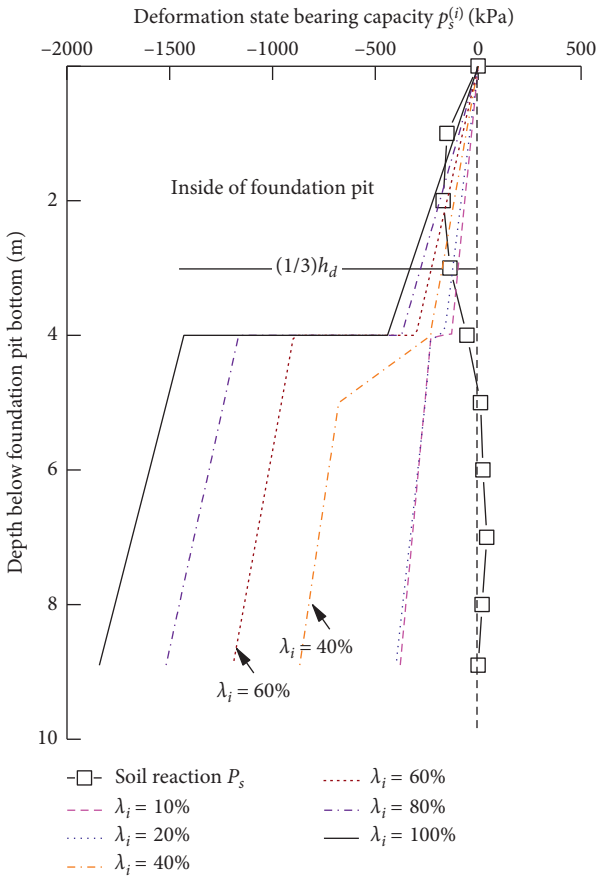

Figure 4: Curve of the relationship between the deformation state bearing capacity $p_s^{(i)}$ and the soil reaction p_s.

Table 5: Internal friction angle φ of the soil.

No.	*a*	*b*	*c*	*d*	*e*	*f*	*g*
φ (°)	45	40	35	30	25	20	15

displacement of the foundation, the substratum foundation is set as an elastic body.

4.2. Establishment of the Analytical Model. The basic model of numerical calculation is shown in Figure 8. In detail, the distributed load q outside the foundation pit corresponds to the geostatic stress of the soil layer above the foundation pit bottom in the calculation example. The shear force at the top of the pile row arises from the difference between the prestress of the anchor cable and the active earth pressure outside the foundation pit. Considering that if the shear force is treated as a concentrated load, the stress will be concentrated on the top of the pile row and affect the analysis result, the shear force is therefore made equivalent to an inverted triangular distribution form and is distributed along the full length of the pile row in the anchorage section. The bending moment at the top of the pile row is the difference between the prestress of the anchor cable, the active earth pressure outside the foundation pit and the point of action of the resultant force.

4.3. Analysis of the Numerical Calculation Results. The aim of this numerical analysis is to determine the plastic zone development range of the soil in the anchorage section inside the foundation pit at different internal friction angles. In the finite element numerical analysis, the plastic zone conceptually means that the soil enters the plastic state in part or in whole when the stress state at a certain point of the soil exceeds the strength envelope of the soil itself. When the soil mass reaches the plastic state, a plastic zone emerges. According to the concept of the plastic zone, the development depth of the plastic zone for anchor piles can be accurately evaluated by extracting the horizontal (normal) stress of the interface around the pile. Specifically, as shown in Figure 9, in the finite element numerical analysis, it is necessary to set an interface element around a pile structure to ensure the coordinated deformation of the pile and soil.

As the anchoring section inside the foundation pit generates a passive earth pressure under the outside earth pressure, the interfacial normal stress is consistent with the passive earth pressure. Therefore, by comparing the extracted interfacial normal stress with the theoretical value of the Rankine passive earth pressure, if the interfacial normal stress is greater than or equal to the Rankine theoretical value, a plastic failure zone forms.

4.4. Analysis of the Plastic Zone Development Range in the Anchorage Section. With the internal friction angle φ as a variable, the interfacial normal stress inside the foundation pit of the anchorage section is extracted in a numerical simulation and compared with the Rankine theoretical value, as shown in Figure 10.

As seen from Figure 10(a), when $\varphi = 15^\circ$, the stress level of the soil in the anchorage section reaches 100% in the depth range of 0–3.7 m below the bottom of the foundation pit. Therefore, it can be determined that the maximum plastic zone development depth of the soil in the anchorage section is approximately 0.42 times the length of the anchorage section, and the soil inside the foundation pit essentially reaches the limit state. The distribution of plastic failure points obtained by numerical calculation is shown in Figure 11.

As seen from Figure 10(b), when $\varphi = 20^\circ$, the stress level of the soil in the anchorage section reaches 100% in the depth range of 0–3.4 m below the bottom of the foundation pit. Therefore, it can be determined that the maximum plastic zone development depth of the soil in the anchorage section is approximately 0.38 times the length of the anchorage section, and the soil inside the foundation pit essentially reaches the limit state. The distribution of plastic failure points obtained by numerical calculation is shown in Figure 12.

As seen from Figure 10(c), when $\varphi = 25^\circ$, the stress level of the soil in the anchorage section reaches 100% in the depth range of 0–4 m below the bottom of the foundation pit. Therefore, it can be determined that the maximum plastic zone development depth of the soil in the anchorage section is approximately 0.56 times the length of the anchorage section, and the soil inside the foundation pit

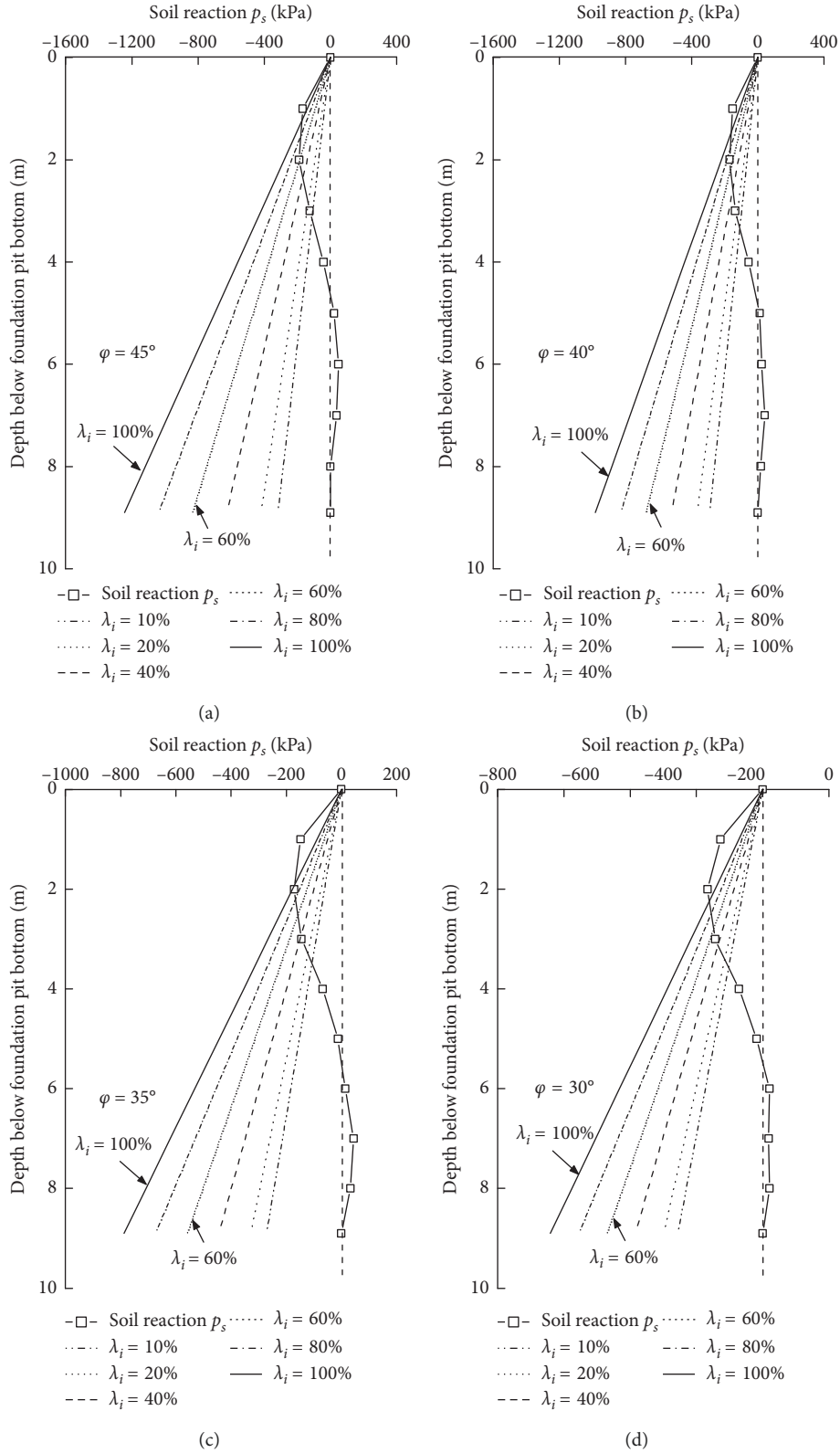

Figure 5: Continued.

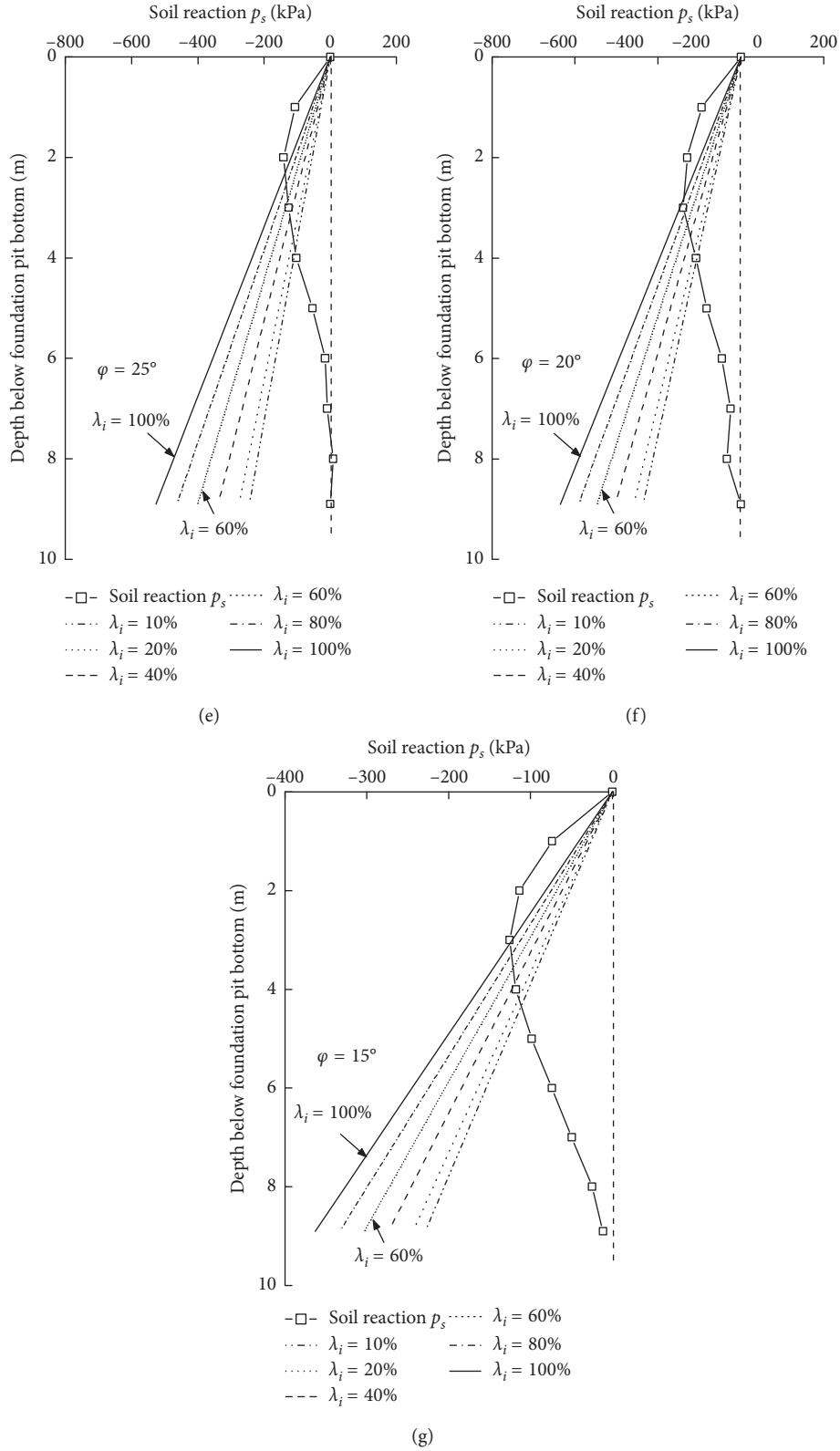

Figure 5: Soil reaction and deformation state bearing capacity of the built-in section at different internal friction angles: (a) $\varphi = 45^{\circ}$, (b) $\varphi = 40^{\circ}$, (c) $\varphi = 35^{\circ}$, (d) $\varphi = 30^{\circ}$, (e) $\varphi = 25^{\circ}$, (f) $\varphi = 20^{\circ}$, and (g) $\varphi = 15^{\circ}$.

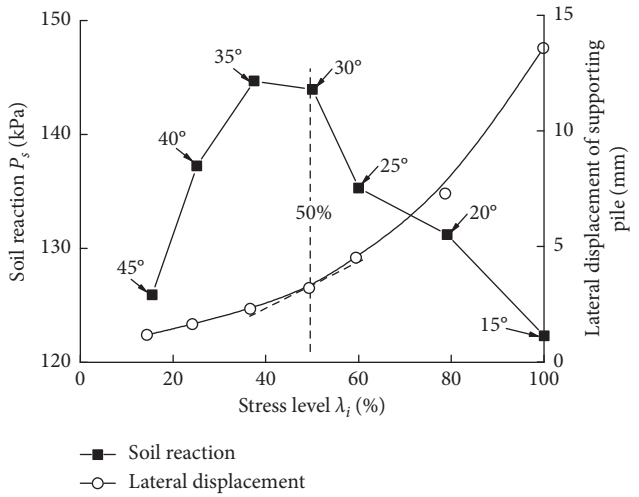

Figure 6: Curve of the relationship between the soil reaction and lateral displacement of the supporting pile at $(1/3)h_d$ and the stress level λ_i.

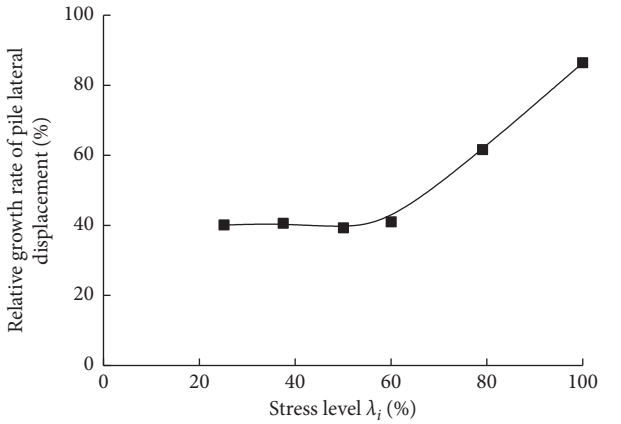

Figure 7: Relation curve between the relative growth rate of the pile lateral displacement and the stress level.

essentially reaches the limit state. The distribution of plastic failure points obtained by numerical calculation is shown in Figure 13.

As seen from Figure 10(d), when $\varphi = 30^\circ$, the stress level of the soil in the anchorage section reaches 100% in the depth range of 0–3 m below the bottom of the foundation pit. Therefore, it can be determined that the maximum plastic zone development depth of the soil in the anchorage section is approximately 0.33 times the length of the anchorage section. The distribution of plastic failure points obtained by numerical calculation is shown in Figure 14.

As seen from Figure 10(e), when $\varphi = 35^\circ$, the stress level of the soil in the anchorage section reaches 100% in the depth range of 0–2.8 m below the bottom of the foundation pit. Therefore, it can be determined that the maximum plastic zone development depth of the soil in the anchorage section is approximately 0.31 times the length of the anchorage section. The distribution of plastic failure points obtained by numerical calculation is shown in Figure 15.

Table 6: Physical and mechanical parameters of the model soil.

Name of the soil layer	Nonclayey soil (inside the foundation pit)	Nonclayey soil (outside the foundation pit)	Substratum foundation
Layer thickness (m)	10	10	30
Unit weight γ (kN/m^3)	24	24	24
Constitutive model	M-C	M-C	M-C
Cohesion c (kPa)	1	1	—
Internal friction angle φ (°)	15~45	40	—
Elastic modulus E (MPa)	30	30	100
Poisson's ratio v_{ur}	0.3	0.3	—
Interfacial strength reduction factor R_{inter}	0.9	0.9	—

Table 7: Mechanical parameters of the pile row.

Parameter	Pile diameter (m)	Rigidity of the section (EA)	Flexural rigidity (EI)
Value	1.2	1.5×10^7	1.8×10^6

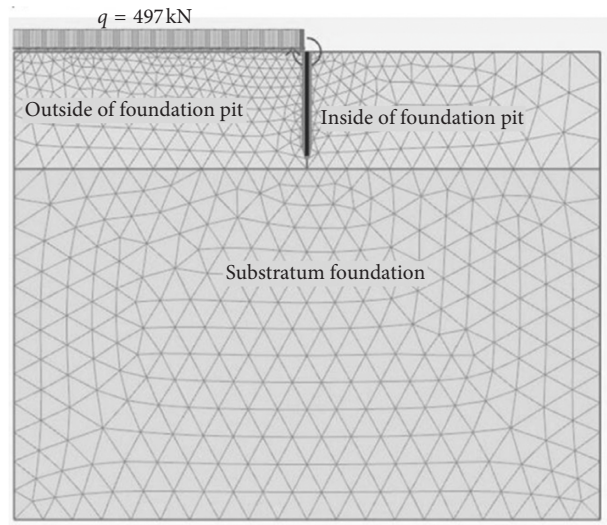

Figure 8: Basic finite element analysis model.

As seen from Figure 10(f), when $\varphi = 40^\circ$, the stress level of the soil in the anchorage section reaches 100% in the depth range of 0–2 m below the bottom of the foundation pit. Therefore, it can be determined that the maximum plastic zone development depth of the soil in the anchorage section is approximately 0.22 times the length of the

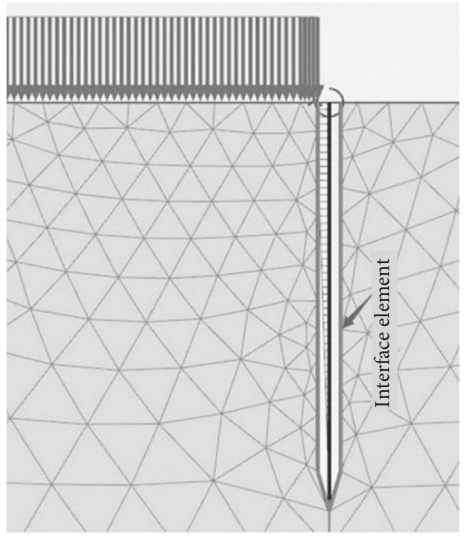

Figure 9: Interface element.

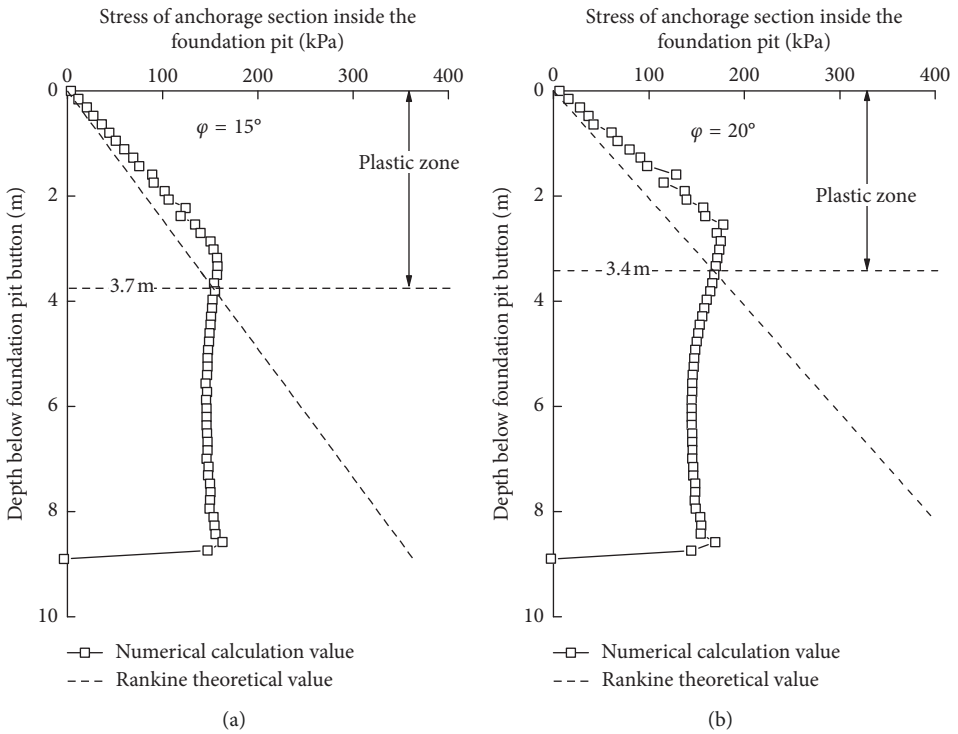

Figure 10: Continued.

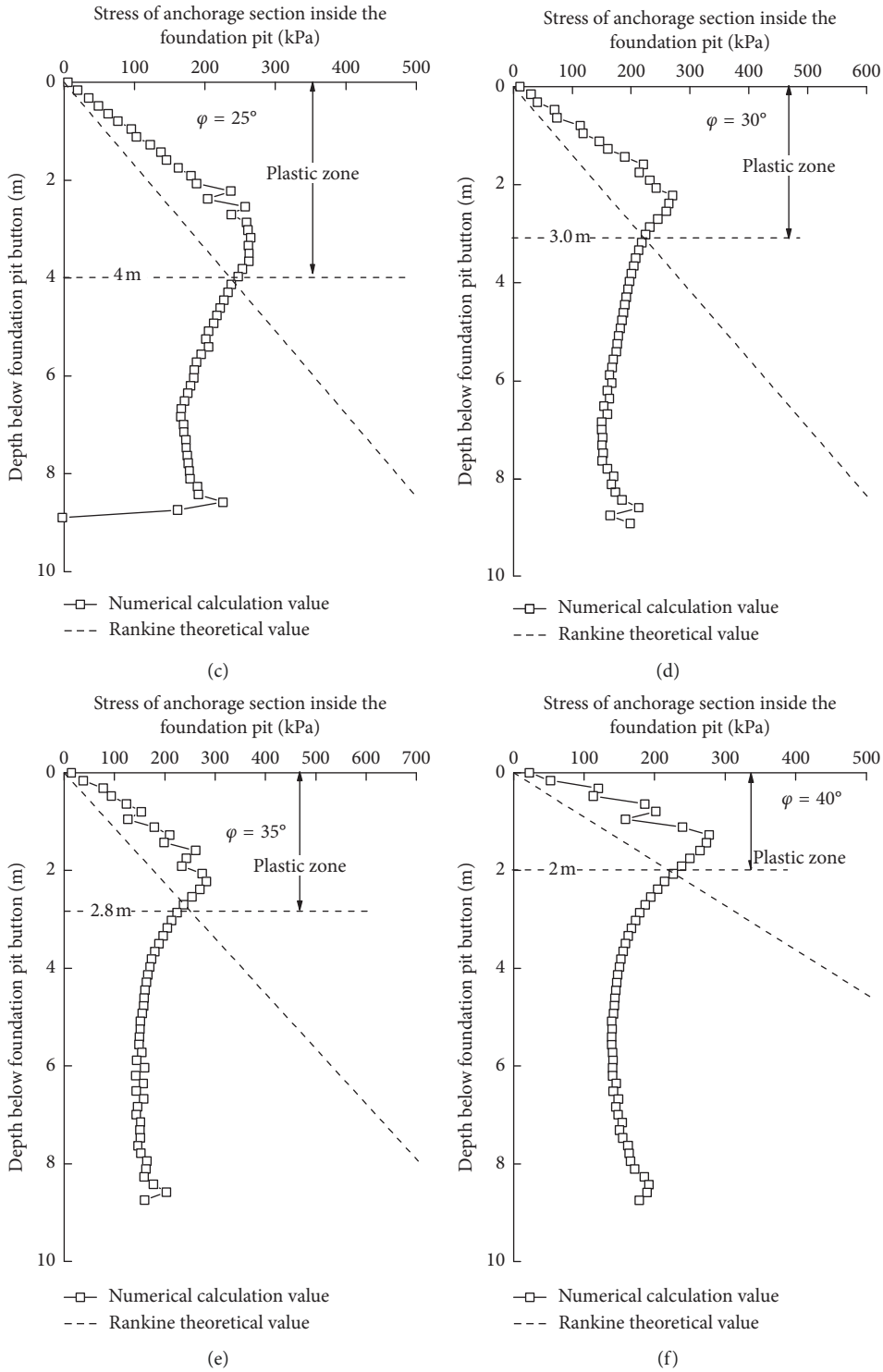

Figure 10: Continued.

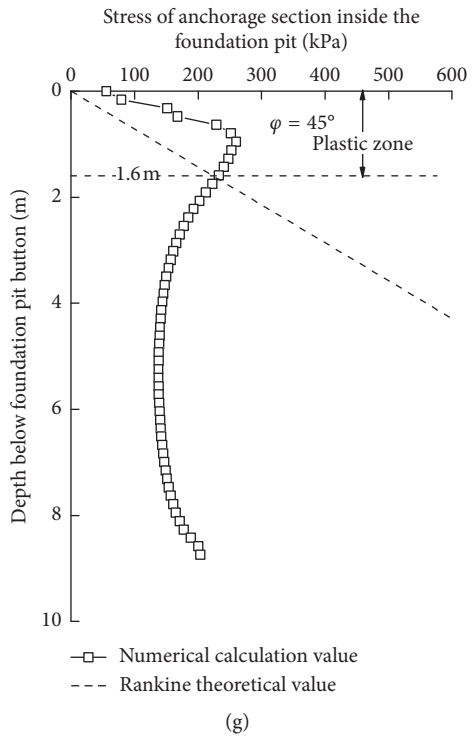

Figure 10: Range of the plastic zone at different internal friction angles φ: (a) $\varphi = 15^{\circ}$, (b) $\varphi = 20^{\circ}$, (c) $\varphi = 25^{\circ}$, (d) $\varphi = 30^{\circ}$, (e) $\varphi = 35^{\circ}$, (f) $\varphi = 40^{\circ}$, and (g) $\varphi = 45^{\circ}$.

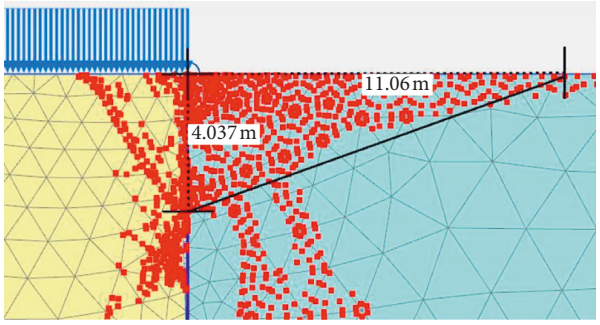

Figure 11: Distribution of failure points inside the foundation pit at $\varphi = 15^{\circ}$.

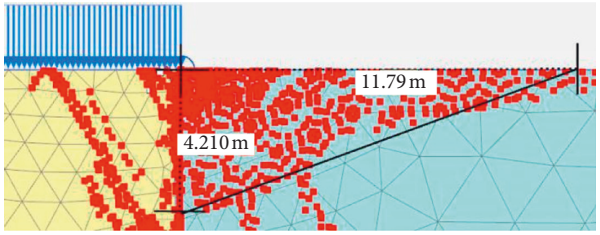

Figure 12: Distribution of failure points inside the foundation pit at $\varphi = 20^{\circ}$.

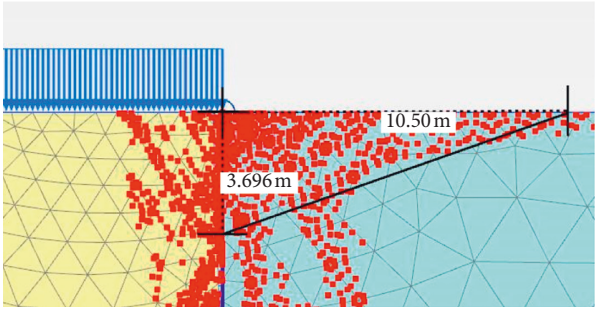

Figure 13: Distribution of failure points inside the foundation pit at $\varphi = 25^{\circ}$.

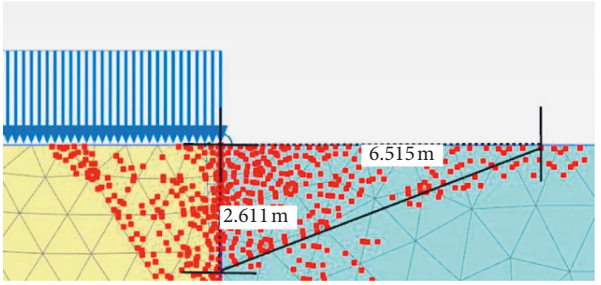

Figure 14: Distribution of failure points inside the foundation pit at $\varphi = 30^{\circ}$.

anchorage section. The distribution of plastic failure points obtained by numerical calculation is shown in Figure 16.

As seen from Figure 10(g), when $\varphi = 45^{\circ}$, the stress level of the soil in the anchorage section reaches 100% in the depth range of 0–1.6 m below the bottom of the foundation pit. Therefore, it can be determined that the maximum plastic zone development depth of the soil in the anchorage

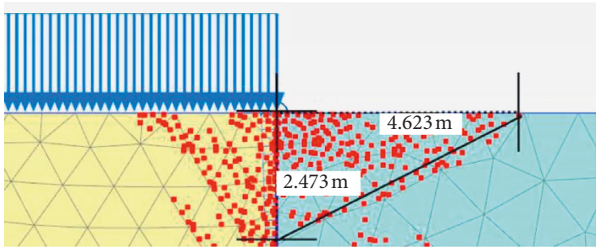

Figure 15: Distribution of failure points inside the foundation pit at $\varphi = 35^{\circ}$.

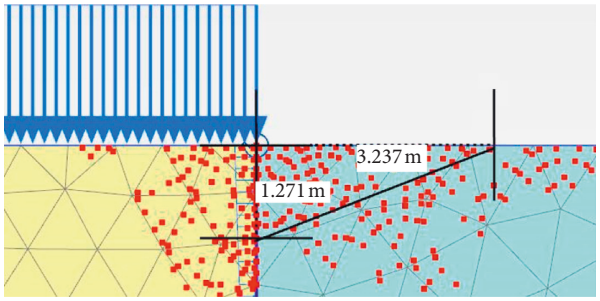

Figure 16: Distribution of failure points inside the foundation pit at $\varphi = 40^{\circ}$.

section is approximately 0.18 times the length of the anchorage section. The distribution of plastic failure points obtained by numerical calculation is shown in Figure 17.

The relationship between the plastic zone development depth obtained by numerical calculation and the internal friction angle is shown in Figure 18.

Since the stress level at the internal friction angle of 45° essentially represents the limit value of most nonclayey soil, the internal friction angles of 15°, 20°, 25°, 30°, 35°, and 40° correspond to a reduction coefficient λ_i of 63%, 52%, 40%, 29%, and 9%, respectively. Therefore, based on the reduction coefficient of 30%–60% in the slowly stable deformation state, it is reasonable to take $(1/3)h_d$ below the bottom of the foundation pit as the checkpoint of the bearing capacity in the slow stabilization state.

5. Evaluation of Social and Economic Benefits

The study of the design method for the deformation state control of the pile-anchor structure of a deep foundation pit is carried out to control the deformation of the foundation pit and its development over time at the design stage and ensure the safety of the foundation pit and surrounding buildings (structures). The economic and social benefits of the study are as follows:

5.1. Analysis of Social Benefits. Based on the checkpoint of the bearing capacity for the slow deformation state in the passive zone of the foundation pit, the deformation of the foundation pit can be controlled purposefully and effectively and stabilized, and the safety of the foundation pit and surrounding buildings (structures) is improved, providing a social benefit.

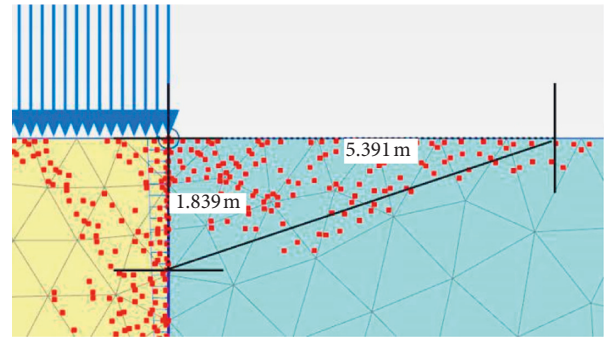

Figure 17: Distribution of failure points inside the foundation pit at $\varphi = 45^{\circ}$.

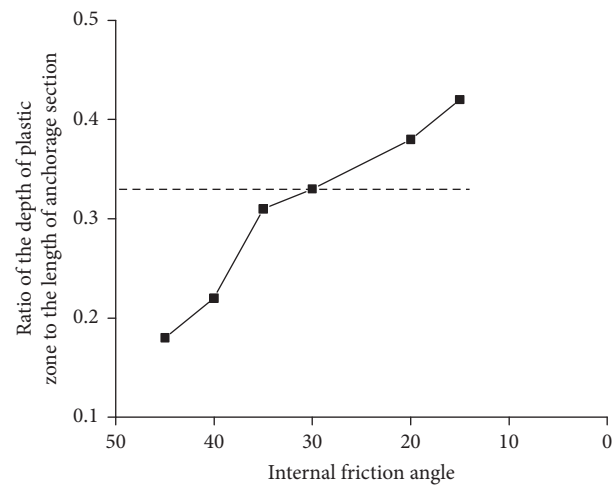

Figure 18: Relationship between the plastic zone development depth and internal friction angle.

5.2. Analysis of Economic Benefits. The original design is optimized based on the checkpoint of the bearing capacity for the slow deformation state in the passive zone of the foundation pit to reduce the engineering cost. Specifically, in engineering design, the embedded depth of piles and the length of anchor rods (cables) can be reduced to reduce the overall cost and bring prominent economic benefits. In addition, the lateral deformation of the foundation pit is controllable, and safety and stability can be ensured.

In summary, the design method for the deformation state control of pile-anchor structures can greatly reduce the engineering cost while ensuring the stability and safety of foundation pits.

6. Conclusion

In this paper, the design method for the pile-anchor structure of a deep foundation pit based on deformation design is established based on the strength parameters of the soil deformation state and the stress mode of the pile-anchor structure. Furthermore, a method for unifying the limit value of the soil plastic development and the checkpoint of the soil deformation state in the passive zone of the deep

foundation pit is proposed. The key technologies and the main conclusions are as follows:

(1) Key technology: this paper expounds the expression of a design method for deformation state control of the pile-anchor structure, the determination and value of key parameters in the design method of deformation state control, and the determination of the checkpoint of the deformation state bearing capacity.

(2) The example calculation shows that with a decreasing internal friction angle φ, the soil strength of the built-in section inside the foundation pit decreases, the plastic zone range of the soil in the built-in section gradually expands, and the maximum development depth of the plastic zone is extended from $0.11h_d$ below the bottom of foundation pit to $0.33h_d$ (h_d is the length of the built-in section). In addition, the requirement that "the resultant soil reaction shall not be greater than passive earth pressure" in JGJ120-2012 *Technical Specification for Retaining and Protection of Building Foundation Excavations* is slightly ambiguous. In view of the requirements for the deformation state control of a deep foundation pit, while the soil in the built-in section inside the foundation pit meets this requirement, the development depth of the plastic zone should still be limited to no more than $(1/3)h_d$, and $(1/3)h_d$ can be taken as the checkpoint of the soil deformation state.

(3) In view of the characteristics of deep foundation pit support engineering, the soil in the built-in section inside the foundation pit should be controlled in a slow stabilization state. In combination with the stress mode of the pile-anchor structure and the strength parameters of the soil deformation state, a design method for the pile-anchor structure when the soil deformation in the built-in section is in a slow stabilization state is established. Moreover, the stress level threshold $\lambda^{(2)}$ corresponding to the slow stabilization state is determined as 30%–60% based on the curve characteristics of the relationship between the soil deformation in the built-in section $(1/3)h_d$ below the bottom of the foundation pit and the stress level.

(4) Based on the stress mode and deformation control requirements of the anchorage section of the pile-anchor structure and the Mohr–Coulomb strength criterion, the deformation state control design method of the pile-anchor structure is established by taking the deformation state bearing capacity at $(1/3)$ h_d of the length of the anchorage section below the bottom of the foundation pit as the checkpoint and the corresponding stress level threshold $\lambda^{(2)}$ of the slow stabilization state.

Data Availability

The data used to support the findings of this study are available from the corresponding author upon request.

Conflicts of Interest

The authors declare that there are no conflicts of interest regarding the publication of this paper.

Acknowledgments

This study was financially supported by non-destructive testing and engineering calculation of bridges for Key Universities in Sichuan Province (Grant no. 2016QYY04).

References

[1] C. C. Vyalov, *The Rheological Principle Of Soil Mechanics*, Science Press, Beijing, China, 1987.

[2] Tan Tjongkie, "The mechanical problems for long-term stability of underground galleries," *Chinese Journal of Rock Mechanics and Engineering*, vol. 1, no. 1, pp. 1–20, 1982.

[3] Y. Cai and X. Cao, "Study of the critical dynamic stress and permanent strain of the subgrade-soil under the repeated load," *Journal of Southwest Jiaotong University*, vol. 31, no. 1, pp. 1–4, 1996.

[4] S. Werkmeister, A. R. Dawson, and F. Wellner, "Permanent deformation behavior of granular materials and the shakedown concept," *Transportation Research Record: Journal of the Transportation Research Board*, vol. 1757, no. 1, pp. 75–81, 2001.

[5] G. Liu, *Computational Methods of High-Speed Railway Subgrade Structure Design Based on Cumulative Deformation Evolution State control*, Southwest Jiaotong University, Chengdu, China, 2013.

[6] Y. Xiong, L. Zhang, Q. Luo, L. Jiang, and J. Zhu, "Calculating method based on deformation time effect on thickness of compressible stratum in high-speed railway foundation," *Scientia Sinica Technologica*, vol. 44, no. 7, pp. 755–769, 2014.

[7] H. Li, *Study on Lateral Displacement Characteristics and State Control Design Method for Shoulder Sheet-Pile Wall of Ballastless Track in High Speed Railway*, Southwest Jiaotong University, Chengdu, China, 2015.

[8] K. Terzaghi, R. B. Peck, and G. Mesri, *Soil Mechanics in Engineering Practice*, John Wiley and Sons, Inc., New York, NY, USA, 1967.

[9] J. T. P. Yao, "Concept of structural control," *Journal of the Structural Division*, vol. 98, no. 7, pp. 1567–1574, 1972.

[10] J. Liu, G. Liu, and Y. Fan, "Theory and practice of space-time effect in soft soil foundation pit engineering (I)," *Underground Engineering and Tunnels*, vol. 3, pp. 7–12, 1999.

[11] J. Liu, G. Liu, and Y. Fan, "Theory and practice of space-time effect in soft soil foundation pit engineering (II)," *Underground Engineering and Tunnels*, vol. 8, pp. 10–14, 1999.

[12] G. Liu, D. Liu, L. Liu, and W. Diao, "Monitoring and analysis of lateral deformation of retaining wall during bottom excavationin deep pit," *Chinese Journal of Rock Mechanics and Engineering*, vol. 28, no. 2, pp. 4386–4394, 2007.

[13] X.-F. Jiang, G.-B. Liu, W.-L. Zhang, and X.-Y. Li, "Deformation characteristics of ultra-deep foundation pit in Shanghai based on measured data," *Chinese Journal of Geotechnical Engineering*, vol. 32, no. 2, pp. 570–573, 2010.

[14] J. Jia, "The practice of "time and space effect" in soft clay excavations," *Chinese Journal of Underground Space and Engineering*, vol. 1, no. 4, pp. 490–494, 2005.

[15] G. Liu and W. Wang, *Foundation Pit Support Manual*, China Building Industry Press, Beijing, China, 2nd edition, 2009.

[16] K. Terzaghi, *Theoretical Soil mechanics*, Wiley, New York, NY, USA, 1943.
[17] P. W. Rowe, Stroyer, Browzin, and Tschebotarioff, "Anchored sheet-pile walls," *Proceedings of the Institution of Civil Engineers*, vol. 1, no. 1, pp. 27–70, 1952.
[18] W. Wu, S. Xu, J. Zhou, Y. Wu, and G. Qin, "Studies of force and deformation properties considering pile-anchor-soil interaction in deep pits," *Chinese Journal of Rock Mechanics and Engineering*, vol. 20, no. 3, pp. 399–402, 2001.
[19] Z. Ou, *Theory and Practice of Deep Excavation Engineering Analysis Design*, Science and Technology Books Co., Ltd., Taipei, Taiwan, 2003.
[20] The Second Survey and Design Institute of the Ministry of Railways, *Design and Calculation of Anti-slide Piles*, China Railway Publishing House, Beijing, China, 1983.
[21] Y. Zheng and Z. Chen, *Engineering Management of Slope and Landslide*, China Communications Press, Beijing, China, 2nd edition, 2010.
[22] L. Lu, *Deformation Timeliness Analysis of the Middle-Lower Compressive Soil Based on Triaxial Tests*, Southwest Jiaotong University, Chengdu, China, 2013.
[23] H. P. Nguyen, *Timely Shearing Deformation Characteristic of Soil and Long Term Deformation Controlling Technique of Embankment for High Speed Railway*, Southwest Jiaotong University, Chengdu, China, 2014.